Journal of Thermophysics and Heat Transfer
Vol. 21, No. 1, January–March 2007

Role of Random Roughness On Thermal Performance of Microfins

Majid Bahrami*
University of Victoria, Victoria, British Columbia V8W 3P6, Canada
and
M. Michael Yovanovich† and J. Richard Culham‡
University of Waterloo, Waterloo, Ontario N2L 3G1, Canada

DOI: 10.2514/1.22353

Heat transfer in rough circular cylinder microfins is studied and a new analytical model is developed. Assuming Gaussian isotropic surface roughness, it is shown that both cross-sectional and surface areas of microfins increase by increasing roughness. Consequently, an enhancement is observed in the heat transfer rate and thermal performance of microfins. The effect of roughness is more profound in lower convective heat transfer coefficient (natural convection) and/or rougher structures. The present model can be implemented to analyze other geometries such as rectangular and tapered microfins.

Nomenclature

A_c = cross-sectional area, m^2
A_s = surface area, m^2
a = mean radius of rough microfin, m
D = mean diameter of rough microfin, m
h = convection heat transfer coefficient, W/m^{2}K
k = fin thermal conductivity, W/mK
k_f = fluid thermal conductivity, W/mK
L = microfin length, m
m_s = mean absolute surface slope [−]
Nu_D = Nusselt number hD/k_f [−]
Q = heat flow rate, W
q = heat flux, W/m^2
R_f = fin thermal resistance, K/W
r = microfin radius, m
T = temperature, K
ϵ = relative roughness, σ/a
ζ = nondimensional length, x/L
θ = nondimensional temperature
$d\Lambda$ = length of surface element, m
σ = roughness standard deviation, m

Subscripts

x = in longitudinal direction
θ = in angular direction
∞ = ambient
0 = reference value, base, smooth microfin

I. Introduction

THERMAL phenomena play a key role in a variety of applications in micro-electro-mechanical systems (MEMS) such as thermal actuators in RF devices [1], thermal flexture actuators [2], and thermal-compliant microactuators [3]. Micropin fin heat exchangers are being used in advanced thermal management solutions ranging from cooling of gas turbine blades [4] to microelectronic chips [5].

According to Brown [6], there are several MEMS fabrication techniques currently in widespread use, including bulk micromachining, surface micromachining, fusion bonding, and LIGA which is a composite fabrication procedure of lithography, electroforming, and molding. The polycrystalline silicon substrates used in micromechanical devices are often rough. Moreover, atomic force microscopy (AFM) images revealed that the surfaces manufactured by MEMS technologies have some level of roughness [7]. The level of this surface roughness depends extensively on the fabrication process used and material properties. The importance of surface roughness becomes more significant as the dimensions of microstructures decrease. This surface roughness can be envisioned as extended surface on the original extended surface.

The heat transfer augmentation due to the presence of surface roughness has been experimentally investigated by several researchers. Achenbach [8] showed through experiments that the heat transfer from a circular cylinder to the crossflow of air increases as a result of surface roughness. He used knurling to create artificial roughness on the cylinders studied; all of his experiments were conducted at high Reynolds numbers, that is, turbulent flow regime. Wang et al. [9] experimentally studied natural convection in air over a uniformly heated, vertical surface covered with microgrooved films. *V* grooves with depths of 18 to 150 μm were used. Their data [9] showed that natural convection was enhanced by up to 20% when microgrooves were used. Honda and Wei [5] conducted experiments and studied the effect of roughness on micropin fins on the boiling heat transfer from a silicon chip immersed in a pool of FC-72. They used square pin fins; the dimensions were $50 \times 50 \times 60$ μm^3 with a surface roughness on the order of 25–35 nm. They reported that the pin fin with higher roughness showed a higher thermal performance [5].

As briefly reviewed, existing experimental studies point out an increase in the fin thermal performance when surface roughness exists. However, to the authors' knowledge, there are no analytical models in the literature that predict this empirically observed trend. This work is an attempt to develop an analytical model to predict the effect of roughness on the thermal performance of circular cylinder microfins. The term *roughness* has been used to refer to a variety of surface treating/irregularities in the thermal-fluid literature, for example, knurling [8] and *V* grooves [9]. However, in this study, we focus only on *random* or *isotropic* (Gaussian) roughness which can be thought of as surface deviations from its nominal topography.

Received 9 January 2006; revision received 31 March 2006; accepted for publication 3 April 2006.

*Assistant Professor, Department of Mechanical Engineering. Member AIAA.
†Professor Emiretus. Fellow AIAA.
‡Associate Professor, Director MHTL.

The results of the analysis provide a better understanding about the effect of roughness on thermal design of microfins and other microstructures.

II. Heat Transfer from Extended Surfaces

The term extended surface or fin is commonly used to refer to a solid that experiences energy transfer by conduction within its boundaries, as well as energy transfer by convection between its boundaries and the surroundings. The main goal of this work is to investigate effect(s) of surface roughness on thermal performance of microfins. One approach is to assume that input parameters of the fin, such as convective heat transfer coefficient and thermal conductivity are constant. Then by systematically varying surface roughness, one can study the effects of roughness on thermal performance of the microfin. The following summarizes the assumptions of the present model for a rough extended surface shown in Fig. 1:

1) heat conduction is one dimensional, that is, in the longitudinal x direction;

2) the fin surface is rough with an isotropic Gaussian distribution of heights;

3) negligible radiation from the surface and no heat source in the fin;

4) uniform heat transfer coefficient, h;

5) constant solid thermal conductivity including surface asperities, k;

6) steady-state conditions.

The errors associated with one-dimensional heat transfer, isotropic conductivity, and constant convective heat transfer coefficient assumptions are insignificant because the dimensions of microfins are very small (on the order of microns). We also assume that the surrounding fluid is a continuum and neglect rarefaction and slip effects. The value of the Knudsen number determines the degree of rarefaction of a gas and the validity of the continuum (gas) flow assumption. For $Kn < 10^{-2}$, the continuum hypothesis is appropriate and the flow can be described by the Navier–Stokes equations using conventional no-slip boundary conditions.

Applying conservation of energy to the differential element shown in Fig. 1, one obtains [10]

$$\frac{d^2T}{dx^2} + \frac{1}{A_c}\frac{dA_c}{dx}\frac{dT}{dx} - \frac{1}{A_c}\frac{h}{k}\frac{dA_s}{dx}(T - T_\infty) = 0 \tag{1}$$

where Eq. (1) provides a general form of the energy balance for one-dimensional, steady-state heat flow in an extended surface. It should be noted that the thermal conductivity of the structure is assumed to be isotropic which means the same thermal conductivity for bulk and asperities. For most applications where rms roughness is small, this assumption is valid. However, for larger values of surface roughness, thermal conductivity values near the surface may be noticeably degraded, depending upon the material and the fabrication process.

The terms A_c, dA_c/dx, and dA_s/dx in Eq. (1) are functions of surface roughness. In the next sections, we will derive relationships for estimating these parameters.

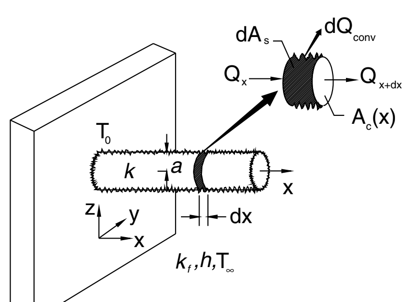

Fig. 1 Energy balance for an extended rough surface.

III. Surface Roughness

According to Liu et al. [11] five types of instruments are currently available for measuring the surface topography: 1) stylus-type surface profilometer, 2) optical (white-light interference) measurements, 3) scanning electron microscope (SEM), 4) atomic force microscope (AFM), and 5) scanning tunneling microscope (STM). Surface texture is most commonly measured by a profilometer, which draws a stylus over a sample length of the surface. A datum or centerline is established by finding the straight line or circular arc in the case of round components, from which the mean square deviation is a minimum. When the surface is Gaussian, the standard deviation σ is identical to the rms value [12], R_q.

$$\sigma = R_q = \sqrt{\frac{1}{l}\int_0^l z^2(x)dx} \tag{2}$$

where l is the sampling length in the x direction and z is the measured value of the surface heights along this length. m_s can be determined across the sampling length from the following:

$$m_s = \frac{1}{l}\int_0^l \left|\frac{dz(x)}{dx}\right| dx \tag{3}$$

IV. Rough Micropin Fins

Consider a rough micropin fin with a mean radius of a and length L; see Figs. 2 and 3. As shown schematically in the figures, roughness of the fin is assumed to possess a Gaussian distribution in both angular and longitudinal directions. It should be noted that the slopes of surface asperities m_s are exaggerated. In reality, the surface asperities can be visualized as shallow hills and valleys, that is, small surface slopes.

Owing to the random nature of roughness, an exact value of the local radius r cannot be used to specify the radius of rough microfins. Instead, probabilities of different radii occurring should be computed. A random variable p is used to represent the deviation of the local radius r in the angular direction, Fig. 2. The standard deviation of p is the surface roughness σ_θ and has the following Gaussian

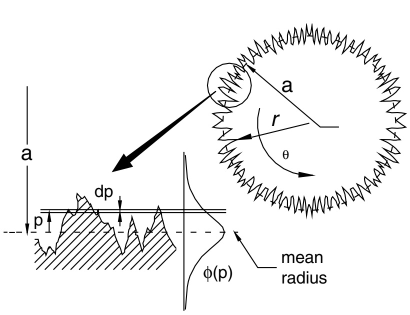

Fig. 2 Cross section of rough pin fin, Gaussian roughness.

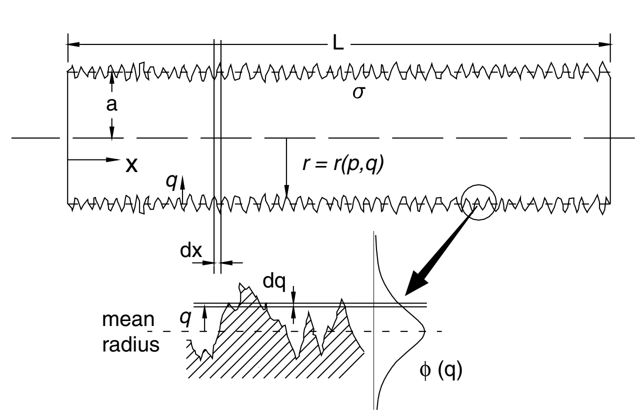

Fig. 3 Longitudinal cross section of random rough pin fin.

distribution:

$$\phi(p) = \frac{1}{\sqrt{2\pi}\sigma_\theta} \exp\left(-\frac{p^2}{2\sigma_\theta^2}\right) \tag{4}$$

The local radius can vary over a wide range of values from much larger to much smaller radii than the mean radius a, valleys and hills in figures, with the Gaussian probability distribution shown in Eq. (4).

The fin surface also has roughness in the longitudinal direction x; see Fig. 3. The variation of the local radius of the microfin r in the longitudinal direction is shown by another random variable q, with the same Gaussian distribution as in the angular direction.

$$\phi(q) = \frac{1}{\sqrt{2\pi}\sigma_x} \exp\left(-\frac{q^2}{2\sigma_x^2}\right) \tag{5}$$

The local radius of the microfin can be written as

$$r = a + p + q \tag{6}$$

where a is the mean statistical value of the local radius r over the cross sections along the entire length L of the microfin.

To better understand Eq. (6), consider cross sections of a rough microfin at different longitudinal locations, Fig. 3. These cross sections can have different mean radii where the probability of these radii occurring can be determined from Eq. (5), $a + q$. Meanwhile, the actual radius at each cross section varies around the mean radius $a + q$ in the angular direction (variations of p) with the probability distribution described in Eq. (4). Therefore, the local radius of a microfin r is a function of both random variables p and q, that is, $r = r(p, q)$. We assume that the local radius is the superposition of the two random variables, as shown in Eq. (6). Note that the variables p and q are independent. For argument sake, consider an imaginary case where a microfin has roughness only in the angular direction; thus one can write $r = r(p)$. As a result, an average of these variables $[r = a + (p + q)/2]$ does not provide a correct answer.

In the general case, the standard deviations σ_θ and σ_x can be different; however, in this study, we assume an isotropic roughness; thus, $\sigma_\theta = \sigma_x = \sigma$.

A. Cross-Sectional Area, A_c

The cross-sectional area of a circular cylinder micropin fin can be calculated from $A_c = \pi r^2$; using Eq. (6), it can be written

$$A_c = \pi \int_{-\infty}^{+\infty} \int_{-\infty}^{+\infty} (a + p + q)^2 \phi(p)\phi(q) \mathrm{d}p \mathrm{d}q \tag{7}$$

Equation (7) considers the probabilities of all values of radius r occurring according to the Gaussian distribution. It should be noted that it is mathematically possible for the variables p and q to have values ranging from $-\infty$ to $+\infty$; see Eqs. (4) and (5). However, the probability of occurring much larger/smaller radii than the mean radius a is quite small.

After a change of variables ($u = p/\sigma$ and $v = q/\sigma$) and simplifying, Eq. (7) becomes

$$A_c^* = \frac{A_c}{A_{c,0}} = \underbrace{\frac{1}{2\pi} \int_{-\infty}^{+\infty} \int_{-\infty}^{+\infty} (1 + \epsilon u + \epsilon v)^2 e^{-u^2/2} e^{-v^2/2} \mathrm{d}u \mathrm{d}v}_{\text{effect of roughness on cross-sectional area}} \tag{8}$$

where A_c^*, $A_{c,0} = \pi a^2$, and ϵ are the normalized cross-sectional area, cross-sectional area of the smooth microfin, and the relative surface roughness, respectively,

$$\epsilon = \frac{\sigma}{a} \tag{9}$$

Note that ϵ is defined as the rms surface roughness over the *radius* of the fin. Equation (8) calculates an *effective* cross-sectional area for a rough pin fin. After solving the integral, one finds

$$A_c^* = \frac{A_c}{A_{c,0}} = 1 + 2\epsilon^2 \tag{10}$$

As expected, the effect of surface roughness is to increase the cross-sectional area of a rough fin. Notice that at the limit where roughness goes to zero $\epsilon \to 0$ (smooth surface), $A_c^* \to 1$.

B. Surface Area, A_s

The differential lateral surface area of a rough micropin fin can be found from

$$\mathrm{d}A_s = r \mathrm{d}\theta \mathrm{d}\Lambda \tag{11}$$

where $r = r(x, \theta)$ and $d\Lambda$ is the statistical mean length of the rough surface element that can be found from

$$\mathrm{d}\Lambda = \int_x^{x+\mathrm{d}x} \sqrt{1 + \left(\frac{\mathrm{d}r}{\mathrm{d}x}\right)^2} \mathrm{d}x \tag{12}$$

It is assumed that the mean absolute surface slope m_s, see Eq. (3), can be used to estimate the statistical mean length of the surface $d\Lambda$, that is,

$$m_s \simeq \frac{\mathrm{d}r}{\mathrm{d}x} \tag{13}$$

It must be noted that the actual local surface slope is a Gaussian parameter which cannot be specified at each element and thus cannot be used in the analysis. As a result, the mean absolute value of surface slope m_s is used as a first degree approximation and a representative value for the entire rough surface. This assumption may have some degree of inaccuracies and may need modification when compared against experimental data. This assumption is consistent with Eq. (1) because the energy balance is for the entire micropin fin. Thus, one may write

$$\mathrm{d}A_s = 2\pi r \sqrt{1 + m_s^2} \mathrm{d}x \tag{14}$$

Averaging Eq. (14) over the microfin length, the mean value of r must be replaced by a, and the effective mean lateral surface area of a rough micropin fin will be

$$A_s = 2\pi a L \sqrt{1 + m_s^2} \tag{15}$$

with $A_{s,0} = 2\pi a L$,

$$A_s^* = \frac{A_s}{A_{s,0}} = \sqrt{1 + m_s^2}$$

Using the same method, one can find $\mathrm{d}A_c/\mathrm{d}x$

$$\frac{\mathrm{d}A_c}{\mathrm{d}x} = 2\pi r \frac{\mathrm{d}r}{\mathrm{d}x} \tag{16}$$

which can be averaged over the microfin and estimated (see the above discussion)

$$\frac{\mathrm{d}A_c}{\mathrm{d}x} \cong 2\pi a m_s \tag{17}$$

The above argument, with regard to the local actual surface slope, also applies to Eq. (17). Substituting Eqs. (10), (14), and (17) in Eq. (1), one finds

$$\frac{\mathrm{d}^2 T}{\mathrm{d}x^2} + \frac{2m_s}{a(1 + 2\epsilon^2)} \frac{\mathrm{d}T}{\mathrm{d}x} - \underbrace{\frac{h}{k} \frac{2\sqrt{1 + m_s^2}}{a(1 + 2\epsilon^2)}}_{m^2 \text{ (fin parameter)}} (T - T_\infty) = 0 \tag{18}$$

where $m^2 = hP/kA_c$ for smooth fins. This ODE can be nondimensionalized in the following form:

$$\frac{d^2\theta}{d\zeta^2} + \alpha\frac{d\theta}{d\zeta} - \beta\theta = 0 \tag{19}$$

where $\theta = (T - T_\infty)/(T_0 - T_\infty)$ and $\zeta = x/L$, and

$$\alpha = \frac{2m_s}{(1+2\epsilon^2)}\left(\frac{L}{a}\right) \qquad \beta = \frac{2hL^2\sqrt{1+m_s^2}}{ka(1+2\epsilon^2)} \tag{20}$$

Note that at the limit of a smooth fin where $\sigma = 0$, $m_s = 0$, and $\epsilon = 0$, Eq. (26) yields the smooth cylindrical uniform cross-section fin equation. The nondimensional parameter β can be written in terms of Nusselt number as follows:

$$\beta = Nu\left(\frac{k_f}{k}\right)\left(\frac{L}{a}\right)^2\frac{\sqrt{1+m_s^2}}{1+2\epsilon^2} \tag{21}$$

where $Nu = hD/k_f$, $D = 2a$, and k_f are the Nusselt number, diameter of microfin, and the fluid thermal conductivity, respectively.

To solve Eq. (19), the following boundary conditions are used:

$$\begin{aligned} \theta = 1 \qquad & \text{at } \zeta = 0 \\ d\theta/d\zeta = 0 \qquad & \text{at } \zeta = 1 \end{aligned} \tag{22}$$

The analytical solution of Eq. (19) with the boundary conditions described in Eq. (22) is

$$\theta(\zeta) = e^{-\alpha\zeta/2}[c_1\sinh(\gamma\zeta) + c_2\cosh(\gamma\zeta)] \tag{23}$$

where $c_2 = 1$ and

$$c_1 = \frac{\alpha\cosh(\gamma) - 2\gamma\sinh(\gamma)}{-\alpha\sinh(\gamma) + 2\gamma\cosh(\gamma)} \quad \text{and} \quad \gamma = \frac{\sqrt{\alpha^2 + 4\beta}}{2} \tag{24}$$

Heat flux at the base of the fin can be found from

$$q_{\text{base}} = -k\frac{T_0 - T_\infty}{L}\frac{d\theta}{d\zeta}\bigg|_{\zeta=0} \tag{25}$$

Using Eq. (23), one can find

$$\frac{d\theta}{d\zeta}\bigg|_{\zeta=0} = \gamma c_1 - \frac{\alpha}{2} \tag{26}$$

Thermal performance of a microfin can be expressed in terms of performance, or efficiency, and or thermal resistance. In this paper, thermal resistance is chosen because of its convenience when used in a thermal resistance network analysis. Considering the difference between the base and the fluid temperature as the deriving potential, a fin resistance R_f is defined as

$$R_f = \frac{T_0 - T_\infty}{Q_f} \tag{27}$$

Fin resistance becomes

$$R_f = \frac{L}{kA_c(\alpha/2 - \gamma c_1)} \tag{28}$$

V. Parametric Study

A parametric study is performed to investigate the effects of surface roughness on different aspects of the thermal performance of micropin fins. Thus some of the physical parameters may have been assumed unrealistically high (or low) to clearly demonstrate the trends. A typical (arbitrary) micropin fin is selected for the study; the input parameters are shown in Figs. 4–6. To better show the effect of roughness, some of the parameters studied are nondimensionalized with respect to their smooth values, that is, $\sigma = 0$.

The effect of surface roughness on the temperature profile of a micropin fin is shown in Fig. 4. The solution is found using Eq. (23). The surface slope m_s may be estimated using an empirical relationship suggested by Lambert and Fletcher [13]

$$m_s = 0.076\sigma^{0.52} \tag{29}$$

where σ is the surface rms roughness in micrometers. The uncertainty of the above correlations is high and use of this correlation is justifiable only where the surface slope is not reported and/or an approximate estimation of m_s is needed [14]. A family of curves are shown in Fig. 4, each corresponding to a relative roughness value in the range of $0 \le \epsilon \le 0.2$, while all other input parameters are kept constant. As shown, the microfin temperature decreases as roughness increases.

The effect of roughness on micropin fin heat flux is shown in Fig. 5. By adding roughness, the fin heat flux increases in microfins. The solution predicts an optimum relative roughness for a microfin

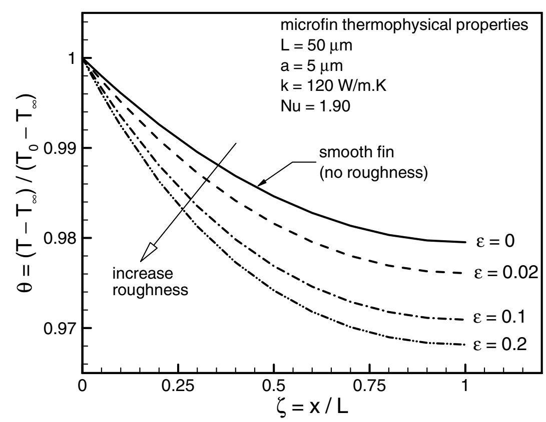

Fig. 4 Effect of surface roughness on temperature profile of pin fin.

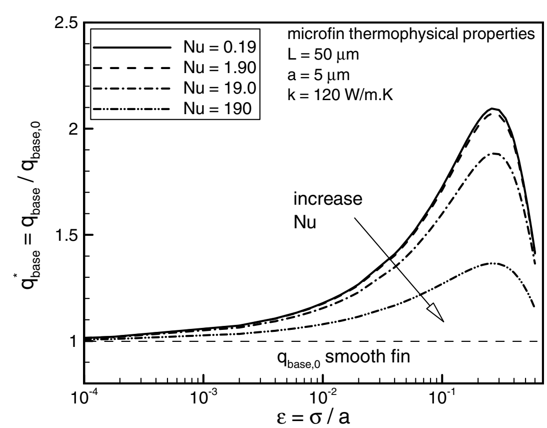

Fig. 5 Effect of roughness on base heat flux of pin fin at various Nusselt numbers.

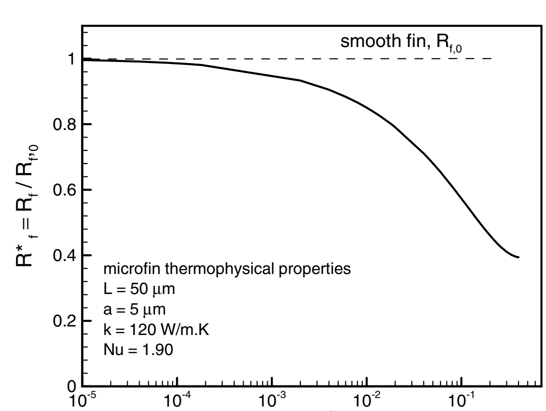

Fig. 6 Effect of roughness on fin thermal resistance.

which maximizes the fin heat flux. This is due to the fact that as roughness increases, the cross-sectional area A_c and surface area A_s both increase according to Eqs. (10) and (15), respectively. These enhancements lead to a higher microfin heat flux. However, the increase in cross-sectional area A_c is larger than the increase in A_s. Although more heat is being conducted into the fin, the increase in surface area is not sufficient to dissipate this heat to the surroundings. It must be noted that this phenomenon is predicted at a large value of relative roughness for the studied microfin, that is, $\epsilon \approx 0.2$ which is not expected to occur in real applications. The optimum surface roughness for a rough micropin fin can be found from

$$\frac{\mathrm{d}q_{\mathrm{base}}}{\mathrm{d}\epsilon} = \frac{\mathrm{d}}{\mathrm{d}\epsilon}\left(\gamma c_1 - \frac{\alpha}{2}\right) = 0$$

where α, γ, and c_1 are functions of roughness and are given in Eqs. (20) and (24).

Figure 5 also shows the effect of the Nusselt number on the nondimensional fin heat flux as a family of curves. It should be noted that the absolute value of fin heat flux increases as the Nusselt number increases; but in Fig. 5 fin heat fluxes are normalized with respect to their smooth values. As the Nusselt number increases, the rate of increase in fin heat flux decreases (curves are flattened). In other words, the rate of increase in fin heat flux due to roughness is more significant at lower values of the Nusselt number, that is, natural convection.

The effects of roughness on thermal resistance R_f of a micropin fin, see Eq. (28), are shown in Fig. 6. The thermal resistance decreases as roughness is introduced to the microfin.

VI. Summary and Conclusions

The effect of random, isotropic surface roughness on microfins is studied and a novel analytical model is developed. The results for circular cylinder micropin fins are presented; however, the proposed model can be implemented to other geometries such as rectangular and tapered microfins. The model can be extended to predict the thermal performance of periodic surfaces with or without roughness.

Two independent random variables are considered to account for deviations of the local radius of rough microfins in the angular and longitudinal directions. The local radius is assumed to be the superposition of the two random variables. Relationships are derived for the temperature distribution, heat flux, and thermal resistance of circular cylinder rough micropin fins.

It is shown that, as a result of roughness, both cross-sectional and surface areas of microfins are increased which result in an enhancement in the heat transfer rate and thus the thermal performance of microfins. Moreover, it is observed that as the surface roughness increases the temperature and thermal resistance of the microfin decrease. The following are found, through analysis:

1) an optimum surface roughness exists that maximizes the fin heat flux,

2) the rate of increase in microfin base heat flux due to roughness is higher at lower Nusselt numbers; thus, better improvement in thermal efficiency of a microfin (due to roughness) can be achieved with a natural convection regime.

For forced convection applications in MEMS and microelectronics cooling, the effect of surface roughness on the thermal performance of microstructures is small but still considerable.

Acknowledgment

The authors gratefully acknowledge the financial support of the Centre for Microelectronics Assembly and Packaging, CMAP, and the Natural Sciences and Engineering Research Council of Canada, NSERC. Our thanks go to K. Narimani for his helpful comments on Sec. IV.

References

[1] Hickey, R., Sameoto, D., Hubbard, T., and Kujath, M., "Time and Frequency Response of Two-Arm Micromachined Thermal Actuators," *Journal of Micromechanics and Microengineering*, Vol. 13, Nov. 2003, pp. 40–46.

[2] Huang, Q., and Lee, N. K. S., "Analysis and Design of Polysilicon Thermal Flexture Actuator," *Journal of Micromechanics and Microengineering*, Vol. 9, 1999, pp. 64–70.

[3] Mankame, N., and Ananthasuresh, G. K., "Comprehensive Thermal Modelling and Characterization of An Electro-Thermal-Compliant Microactuator," *Journal of Micromechanics and Microengineering*, Vol. 11, July 2001, pp. 452–462.

[4] Marques, C., and Kelly, K. W., "Fabrication and Performance of A Pin Fin Micro Heat Exchanger," *Journal of Heat Transfer*, Vol. 126, June 2004, pp. 434–444.

[5] Honda, H., and Wei, J. J., "Enhanced Boiling of FC-72 on Silicon Chips With Micro-Pin-Fins and Submicron-Scale Roughness," *Journal of Heat Transfer*, Vol. 124, April 2002, pp. 383–390.

[6] Brown, E. R., "RF-MEMS Switches for Reconfigurable Integrated Circuits," *IEEE Transactions on Microwave Theory and Techniques*, Vol. 46, No. 11, 1998, pp. 1868–1880.

[7] Maboudian, R., "Surface Processes in MEMS Technology," *Surface Science Reports*, Vol. 30, 1998, pp. 207–269.

[8] Achenbach, E., "The Effect of Surface Roughness on The Heat Transfer From A Circular Cylinder To The Cross Flow of Air," *International Journal of Heat and Mass Transfer*, Vol. 20, March 1977, pp. 359–369.

[9] Wang, T., Mislevy, S. C., and Huang, J. C. P., "Natural Convection Enhancement On Micro-Grooved Surfaces," *Journal of Enhanced Heat Transfer*, Vol. 1, No. 3, 1994, pp. 245–254.

[10] Incropera, F. P., and DeWitt, D. P., *Fundamental of Heat and Mass Transfer*, Wiley, New York, 1996, Chap. 3.

[11] Liu, G., Wang, Q., and Ling, C., "A Survey of Current Models for Simulating Contact Between Rough Surfaces," *Tribology Transactions*, Vol. 42, No. 3, 1999, pp. 581–591.

[12] Johnson, K. L., *Contact Mechanics*, Cambridge Univ. Press, Cambridge, U.K., 1985, Chap. 13.

[13] Lambert, M. A., and Fletcher, L. S., "Thermal Contact Conductance of Spherical Rough Metals," *Journal of Heat Transfer*, Vol. 119, No. 4, 1997, pp. 684–690.

[14] Bahrami, M., Culham, J. R., Yovanovich, M. M., and Schneider, G. E., "Review Of Thermal Joint Resistance Models for Non-Conforming Rough Surfaces in a Vacuum," *Journal of Applied Mechanics* (to be published); also Paper HT2003-47051, 2004.